



Exploring the effectiveness of using internal CNC system signals for chatter detection in milling process

Xiaochen Zheng^{a,*}, Pedro Arrazola^b, Roberto Perez^c, Daniel Echebarria^d,
Dimitris Kiritsis^a, Patxi Aristimuño^b, Mikel Sáez-de-Buruaga^b

^a Swiss Federal Institute of Technology Lausanne (EPFL), Lausanne, 1015, Switzerland

^b Faculty of Engineering - Mondragon Unibertsitatea, Arrasate-Mondragon, 20500, Spain

^c GF Machining Solutions, Biel, 2504, Switzerland

^d Unimetrik S.A., Legutiano, 01170, Spain

ARTICLE INFO

Communicated by Y. Lei

Keywords:

Chatter detection
Milling process
Internal signal
Empirical mode decomposition
Autoencoder

ABSTRACT

Chatter is a harmful self-excited vibration that commonly occurs during milling processes. Data-driven chatter detection and prediction is critical to achieve high surface quality and process efficiency. Most existing chatter detection approaches are based on external sensors, such as accelerometers and microphones, which require installation of extra devices. Some recent studies have proved the feasibility of online chatter detection using internal signals such as drive motor current. This study aims to investigate the effectiveness of different internal signals extracted from CNC system for chatter detection and compare them with external acceleration signals. The external and internal signals are first compared with time–frequency analysis using Discrete Fourier Transform and Ensemble Empirical Mode Decomposition approaches. Two chatter detection methods are then presented based on manually and automatically extracted features respectively. The first method uses two nonlinear dimensionless indicators, C_0 complexity and Power Spectral Entropy, of filtered signals. The second approach uses autoencoder for automatic feature extraction and Support Vector Machine as classifier for chatter identification. A series of milling experiments are conducted and chatters are intentionally created by changing the milling process parameters. Multiple internal signals are collected using software provided by the machine manufacturer. Results show that several internal CNC signals, such as the nominal current signal and the actual torque signal, can achieve comparable performance to external signals for chatter detection.

1. Introduction

Chatter is a type of adverse self-excited vibration of the tool-workpiece couple that widely occurs in milling process. It is usually generated due to the dynamic flexibility of the elements involved in the machining process: the machine tool structure, the spindle, the tool/toolholder, the fixture system or the workpiece to be machined itself. Chatter can damage the surface quality of the finished workpiece, and reduce the tool and spindle lifetime, thus decrease the overall productivity of the manufacturing system. Chatter prediction, detection and suppression has been a critical task for machining-related research and industrial applications.

The most popular chatter detection methods are based on the frequency differences between stable and chatter processes. During stable milling processes, the vibrations and forces are periodic at the tooth passing frequency and its harmonics; whereas when

* Correspondence to: ICT for sustainable manufacturing Group, EPFL, Lausanne, Switzerland
E-mail address: xiaochen.zheng@epfl.ch (X. Zheng).

<https://doi.org/10.1016/j.ymssp.2022.109812>

Received 3 June 2022; Received in revised form 19 August 2022; Accepted 14 September 2022

Available online 26 September 2022

0888-3270/© 2022 The Author(s). Published by Elsevier Ltd. This is an open access article under the CC BY license (<http://creativecommons.org/licenses/by/4.0/>).

chatter occurs, forced vibrations appear not only at the harmonics of the tooth passing frequency, but also at the vicinity of the chattering natural frequency as well as the integer multiples of frequencies away from the chatter frequency [1]. The target of chatter detection is to separate the extra vibrations caused by chatter from periodic vibrations caused by tooth passing. For this target, it is necessary to capture different signals that can reflect the vibrations using robust and practical sensors.

Under the Industry 4.0 context, data-driven online chatter detection enabled by Industrial Internet of Things (IIoT) and machine learning has been widely adopted in many intelligent manufacturing systems. Depending on the data sources, Aslan and Altintas [1] categorized data-driven online chatter detection approaches into direct and indirect approaches:

- The direct approaches detect chatter using signals that are directly generated by the vibrations of the tool-workpiece couple without any filtering or transforming. These signals are usually gathered from external sensors installed directly on the workpiece or cutting tool, such as accelerometers and dynamometers; or sensors placed close to the tool-workpiece couple such as acoustic emission (AE) sensors.
- The indirect chatter detection approaches calculate or estimate the chatter vibration using signals that are not directly generated by the vibrations of the tool-workpiece. These signals are usually collected from adjacent machine components such as force signals from the tool holder or spindle; or from the machine control system such as the current signals from the internal feed drive motor.

The main advantage of the direct approaches is that they are more sensitive and reliable since the signals can directly reflect the characteristics of the vibrations. The direct approaches have been widely applied during the past decades especially with the rapid development of machine learning in recent years. However, there are some drawbacks of these approaches limiting their applications. Firstly, it requires extra installation of sensors which increases cost and may cause inconvenience to the milling operations [2]; moreover, the signals need additional analog–digital converter in some cases which increases the complexity of the system [1]; in addition, the sensors placed near the workpiece, such as microphones and AE sensors, may include ambient noise from the machine or other sources, and they may be amplified at certain frequencies during milling process, which can be classified as chatter, resulting in false chatter alarms [3,4].

Some indirect chatter detection approaches use signals generated by a smart tool holder or spindle, which contains capacitive sensors or force sensors [5,6]. These signals can be used for chatter detection based on the predefined structural dynamic models between the tool holder or spindle and the cutting tool tips. Although such approaches can provide accurate and reliable signals, they are usually expensive and may reduce the dynamic stiffness of the spindle [1]. To cope with the aforementioned drawbacks caused by the installation of costly sensors and smart tool holders or spindles, the inherent signals from the machine control system, such as the drive motor current signal, have been attracting more attention recently as another promising data source for indirectly chatter detection. Previous studies have verified the feasibility of chatter detection using current signals collected from spindle drive motor and CNC system. More details of these studies are introduced in the next section.

The rest of the paper is organized as follows. Section 2 reviews some of the pertinent studies; Section 3 introduces the overall data analysis and chatter detection methods. Section 4 presents a case study, and demonstrates the chatter detection approaches together with the performance evaluation results. Section 5 concludes the paper by summarizing the main contributions and existing limitations.

2. Related work

A recent study [7] reviewed the existing studies about chatter detection and the result shows that most of the studies are using direct approaches based on external sensors. Among them accelerometer [8,9], dynamometer [10,11], microphone [12,13] are the most popular data sources. To capture more features of chatter, some studies [14,15] use multiple types sensors to collect different signals. Despite the high sensitivity and reliability, there are obvious disadvantages of these direct approaches. For example, force sensors are usually bulky and expensive, and their installation range has limitations [16]; microphones are limited by installation location, operating mode, and they are sensitive to environmental noise [17].

In addition to the external sensors, some integrated capacitive and force sensors in advanced machine components also provide signals for indirect chatter detection. A smart tool holder containing capacitive sensors was developed in [5], which enables four-component cutting force measurement in milling process. A Spindle Integrated Force Sensor (SIFS) system was presented in [6] which integrates Piezo-electric force sensors into the stationary spindle housing for cutting force measurement with dynamic compensation. The collected force signals can be used for chatter detection based on the predefined structural dynamic models between the tool holder or spindle and the cutting tool tips. Although such approaches can provide accurate and reliable signals, they are usually expensive and may reduce the dynamic stiffness of the spindle [1].

To avoid the installation of costly sensors and smart components, some studies attempt to use signals from built-in machine tools and control systems for chatter detection. Soliman and Ismail [18] explored the feasibility of using spindle drive current signal to detect chatter of a vertical milling machine. They proved that drive current signals can transmit chatter frequencies reliably. Focusing on the turning process, Liu et al. [2] used three current sensors to measure the three-phase current of feed motor in order to detect chatter. Lamraoui et al. [19] presented a chatter detection approach for CNC milling process based on spindle motor current signals collected from the electric cabinet with three hall-effect current clamps. The main limitation of these approaches is the data acquisition method which still relies on additional sensors or equipment.

The inherent drive motor current signal has been attracting more attention in recent years since it avoids additional sensors or equipment of the machining system. A disturbance observer theory–based method was proposed in [20,21]. A disturbance

Table 1
Internal signals captured from Heidenhain TNC 640 CNC.

Signals	Description	Axis	Frequency
a act	Actual axis acceleration value [m/s^2] or [$^\circ/\text{s}^2$], calculated via the position encoder. Actual spindle acceleration value [rpm/s], calculated via the speed encoder.	X, Y, Z	1/3 kHz
v act	Actual axis feed rate [mm/min] or [$^\circ/\text{min}$], calculated via the position encoder. Actual spindle speed value [rpm], calculated via the speed encoder.	X, Y, Z	1/3 kHz
s act	Actual position [mm] or $^\circ$ with respect to the machine coordinate system M-CS	X, Y, Z	1/3 kHz
M actual	Actual torque value [N m]	X, Y, Z, S1	10 kHz
I N int	Integral-action component of nominal current value [A]	X, Y, Z, S1	10 kHz
Accelerometer	Acceleration [m/s^2] captured from external accelerometer installed to the workpiece	X, Y, Z	3.24 kHz

observer enables using only the servo information of the spindle control system to detect cutting torque variations which cause the chatter. Low-pass filters and case dependent band-pass filters are commonly used to process the captured information to identify the chatter frequency. In order to define the band-pass frequency of the filters, manual intervention is needed to tune the parameters of the filter according to the cutting conditions and structural frequencies of the machine tool and workpiece [1]. To address this limitation, Aslan and Altintas [1] used the readily available CNC drive current commands to detect chatter based on the dynamics of closed spindle velocity controller which is identified with available CNC functions and digital communication features. This method requires a deep understanding of the spindle control system of the machine.

Modern CNC systems can provide rich information about the machining process parameters including the drive current and torque. These signals can be extracted with customized software provided by the machine manufacturer. The aim of this paper is to investigate the effectiveness of different internal signals extracted from CNC system for chatter detection, specifically for the tool-workpiece couple chatter. The external accelerometer signals will be used as benchmark for comparison. Different from previous study [1], this paper aims to avoid analyzing the structural characteristics of the machining system. It will enable data scientists and engineers to implement chatter detection systems even without deep knowledge of the CNC system.

3. Methodology

The overall workflow of this study is illustrated in Fig. 1. Firstly, external acceleration signals and internal CNC signals are gathered from the milling machine and CNC system. Then, the time–frequency analysis is performed using Fast Fourier transform (FFT) and Ensemble Empirical Mode Decomposition (EEMD) approaches. Based on the preliminary analysis results, the obvious insignificant signals are removed and the selected signals are then used for chatter detection. Two chatter detection methods are utilized based on manually extracted features and automatically extracted features respectively. The former method adopts two indicators for identifying chatter, namely the C_0 complexity and Power Spectral Entropy (PSE); whereas the latter uses autoencoder for feature extraction and Support Vector Machine (SVM) for chatter prediction. Finally, the performance of chatter detection between external and internal signals is compared. More details of each step are explained as follows.

3.1. Data acquisition

The milling experiments in this study are conducted with a 5-axis Mikron MILL P800U milling machine manufactured by GF Machining Solutions.¹ The control unit of the machine is Heidenhain TNC 640.² Various signals can be extracted from the Heidenhain CNC system using an accompanying software named TNCscope. These signals represent different perspectives about the milling process on multiple axes such as feed rate, spindle position, motor current, torque and electric power etc. Among these signals, the torque signal and the current signal that controls torque are most relevant to chatter vibrations according to the previous study [18]. They will be the main investigation targets in this paper. In addition, an external MONTRONIX PulseNG accelerometer is attached to the workpiece to directly capture the acceleration signals of the workpiece vibrations, which will be used as benchmark for evaluating the performance of internal signals for chatter detection.

Table 1 lists all the signals captured for this study including their description and sampling frequency. Each signal contains three or four axes. The X , Y and Z axes are the Cartesian axes of the machine, which are related to the linear movement of the tool. The S1 axis is the spindle of the machine related to the rotational axis of the tool. In addition, the main working plane is the X - Y plane, which is perpendicular to the Z axis. The rotational axis of the spindle S1 is parallel to the Z axis. The depth of pass is given in the Z axis during machining.

¹ <https://www.gfms.com/com/en/machines/milling/5-axis/mikron-mill-p-u-series.html>

² <https://www.heidenhain.com/products/cnc-controls/tnc-640>

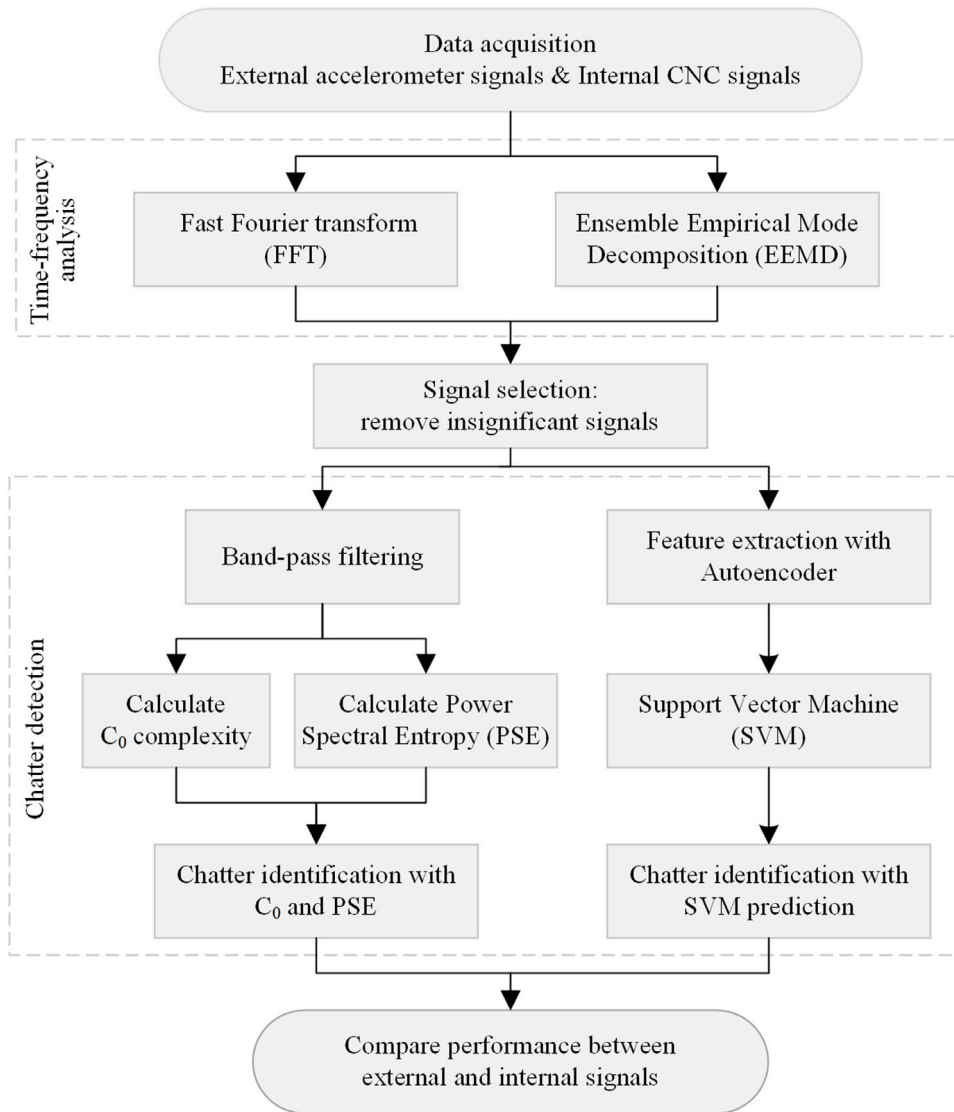


Fig. 1. Workflow for data acquisition and chatter detection.

3.2. Time–frequency analysis

The collected data during the milling process are time series with relatively high frequencies. It is difficult to understand their characteristics directly from the original time domain. Moreover, chatter usually happens at certain frequencies. Therefore, time–frequency analysis is an efficient approach to obtain the key characteristics of the signals.

Fourier analysis is a common approach to convert a time domain signal to a representation in the frequency domain. The discrete Fourier transform (DFT) can decompose a sequence of data into a series of frequency components. FFT accelerates the DFT by factorizing the DFT matrix into sparse factors containing mostly zeros [22]. In this study FFT is used to preliminarily explore the frequency characteristics of the captured signals aiming to identify the chatter frequency ranges.

Empirical Mode Decomposition (EMD) is time–frequency analysis method that can decompose a signal into a set of physically meaningful Intrinsic Mode Function (IMFs) and a residual trend. It is effective for decomposing nonlinear and non-stationary signals since it does not require predefined base functions [23]. However, it suffers from the mode mixing problem which may result in incorrect characteristic information of the signal [24]. The noise-assisted EMD method was then proposed to address this problem by utilizing the Gaussian white noise’s statistical property of uniform distribution to improve the distribution of extreme points in original signal [8,25]. The theoretical foundation and algorithm of EEMD is introduced in [25,26]. In this study, an open source program package named *libeemd* [27] is used to perform the EEMD algorithm.

3.3. Chatter detection methods

Time–frequency analysis provides insights about the key characteristics of the signals in the frequency domain. To implement chatter detection in real applications, it is necessary to extract the key features and represent them with certain indicators. These features can be extracted manually with conventional approaches or automatically with different machine learning methods.

3.3.1. Chatter detection based on conventional feature extraction

Two nonlinear dimensionless indicators, C_0 complexity and PSE, were used in a previous study [8] and proved to be effective for chatter detection. They can properly represent the signal features in time domain and frequency domain respectively.

- C_0 complexity. C_0 complexity is a nonlinear complexity analysis method proposed by Fang et al. [28] and further explored and optimized by En-hua et al. [29] and Cai and Sun [30]. The main advantage of the C_0 complexity method is that it enables a robust estimation with small dataset and does not need coarse graining preprocessing [8]. The aim of the C_0 complexity method is to calculate the proportions of irregular random components in complex time series. It first removes the regular components from the original signal and then calculate the energy ratio of random parts to the original signal. A larger C_0 value represents a higher level of complexity, meaning the signal is closer to random time series.

The calculation of the C_0 complexity is based on FFT, making the computation fast. The key steps of the C_0 complexity algorithm are described as follows:

- (1) For a time series $x(t)$, perform FFT and obtain the Fourier transformation: $F(k) = FFT(x(t))$.
- (2) Calculate the mean square value of $F(k)$:

$$G_N = \frac{1}{n} \sum_{j=1}^n |F(k)|^2 \tag{1}$$

where n is the length of the time series $x(t)$.

- (3) Input a parameter $r(r > 1)$ and keep the spectrum components that are larger than rG_N unchanged, whereas replace the other components with zero:

$$\tilde{F}(k) = \begin{cases} F(k) & \text{if } |F(k)|^2 > rG_N \\ 0 & \text{if } |F(k)|^2 \leq rG_N \end{cases} \tag{2}$$

where $r(r > 1)$ is a given positive constant whose recommended range is 5 to 10 in practical applications.

- (4) Calculate the inverse fast Fourier transform (IFFT) of $\tilde{F}(k)$: $\tilde{x}(t) = IFFT(\tilde{F}(k))$.
- (5) Finally the C_0 complexity is defined as:

$$C_0 = \frac{\sum_{t=1}^n |x(t) - \tilde{x}(t)|^2}{\sum_{t=1}^n |x(t)|^2} \tag{3}$$

The range of C_0 complexity value is a real number between zero and one. It is zero for a constant time series and approaching to zero for a periodic signal. For a stochastic random time series with independent identical distribution and has finite four order moment, the C_0 value converges to one with a probability of one [30].

- *Power spectral entropy*. PSE is a quantitative information entropy that can quantify the spectral complexity of a signal and reflect the uncertainty levels of information [31,32]. It is calculated based on the probability density function of the frequency components of a signal [33]. The key calculation steps of the PSE algorithm [8] are explained as follows:

- (1) For a time series $x(t)$, perform FFT and obtain the Fourier transformation $F(k) = FFT(x(t))$.
- (2) Calculate the power spectrum of the Fourier transformation:

$$s(f) = \frac{1}{2\pi n} |F(k)|^2 \tag{4}$$

where n is the length of the time series $x(t)$.

- (3) Estimate the probability density function of the power spectrum by normalization over all frequency components:

$$P_i = \frac{s(f_i)}{\sum_{i=1}^n s(f_i)}; (i = 1, 2, \dots, n) \tag{5}$$

where P_i is the corresponding probability density of the frequency component f_i , and $s(f_i)$ is its spectral energy.

- (4) Calculate the PSE and normalize it by the factor $\ln(n)$:

$$PSE = \frac{-\sum_{i=1}^n P_i \cdot \ln(P_i)}{\ln(n)} \tag{6}$$

Similar to the C_0 complexity, the range of PSE value is also between zero and one. A larger PSE represents a higher level of uncertainty and the distribution of the frequency components is comparatively even, which means larger proportion of irregular random components in the original signal.

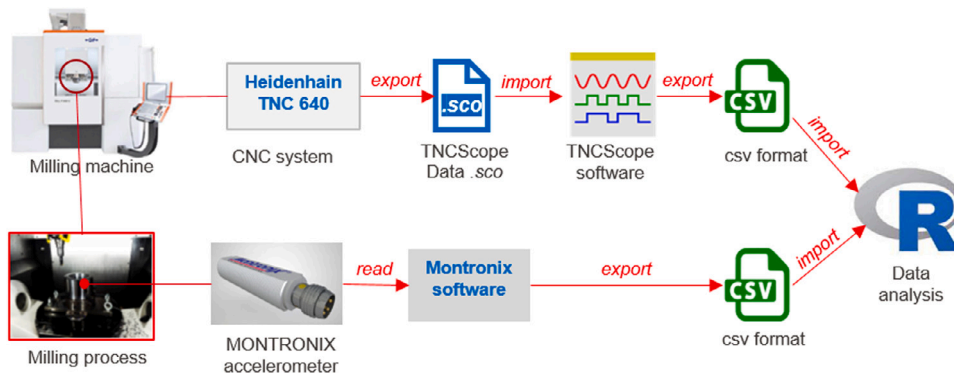


Fig. 2. Experiment setup and data acquisition workflow.

3.3.2. Chatter detection based on automatic feature extraction

The aforementioned conventional manual feature extraction requires profound understanding of the signals through time–frequency analysis. It depends heavily on the experts' domain knowledge. The quick development of machine learning technologies enables automatic feature extraction using algorithms such as autoencoder.

- **Autoencoder.** An autoencoder is a special type of artificial neural network that can learn efficient representations of input information. It is typically composed of an input layer, multiple hidden layers and an output layer. The first half of the network, i.e. the encoder, compresses the input signal into a specified number of dimensions; and the second half, i.e. the decoder, attempts to reconstruct the original signal based on the compressed data. During this encoding–decoding process, the network is trained by reducing the insignificant information from the original signal. It has been widely used for dimensionality reduction and noise removing in many domains. Some recent studies [15,34,35] have also applied it for chatter detection. The output of the encoding layers of an autoencoder network, usually the middle hidden layer, represents the key features of the original signal. It makes autoencoder an efficient approach for automatic feature extraction. These extracted features can be further used as input for supervised learning with algorithms like SVM. An example of such combination for chatter detection was demonstrated in a previous study [15]. The stacked-denoising autoencoder (SDAE) and Adaboost-SVM are used to analyze acceleration signals and achieved promising results even considering samples with wrong labels. This study will follow a similar strategy by replacing the combination of SDAE and Adaboost-SVM with conventional autoencoder and SVM considering the samples in this study are cleaned without wrong labels.

4. Experiments and results

4.1. Experiment setup

A series of experiments are conducted using the aforementioned milling machine to capture the external and internal signals as listed in Table 1. The material of the workpiece is AISI 1100 steel and the size is 80 mm × 80 mm. The dimension of the cutting tool is 25 mm with two cutting edges. The model of the tool holder is Sandvik 490-025A20-08L with Sandvik 490R-08T304E-ML 2030 insert. Six face milling trials are conducted with constant cutting speed (V_c , 250 m/min), spindle rotational speed (n , 3200 rpm) and feed per tooth (f_z , 0.14 mm/z), while the cutting depths (a_p) increases from 0.75 mm to 3.5 mm (0.75 mm, 1.50 mm, 2.00 mm, 2.50 mm, 3.00 mm, 3.50 mm). Each trial is executed with one pass producing a 25 mm × 80 mm slot. As shown in Fig. 3, chatter started to appear at cutting depth 2.50 mm and getting more severe at 3.00 mm and 3.50 mm.

The internal CNC signals and external acceleration signals are collected as depicted in Fig. 2. The milling machine and its CNC system are introduced in the Methodology section. The internal signals are first exported through the control system as TNCScope Data Files (.sco), which are then transformed to CSV formats using the TNCScope software provided by Heidenhain. The external acceleration signals are collected from the MONTRONIX PulseNG accelerometer which are attached to the workpiece. The signals are extracted with the accompanying Montronix software and exported as CSV files. Both internal and external signals are finally imported to RStudio for further analysis.

The roughness and waviness of the machined surfaces are measured using a Mitutoyo SJ 210 roughness tester. Three measurements are performed for each of the machined surfaces. The measurement results are listed in Table 2. As depicted in Fig. 4, in general no significant roughness variations in R_a , R_z , R_t and R_{max} are found between normal and chatter conditions, although the roughness at lower cutting depths seems to be lower. The analysis of the waviness profile shows that chatter affects the waviness parameters, increasing the values of W_a , W_z , W_t and W_{max} significantly.

4.2. Data analysis

The data collected from both the internal CNC system and the external accelerometer during the six machining trials are first investigated in time and frequency domain following the workflow depicted in Fig. 1.

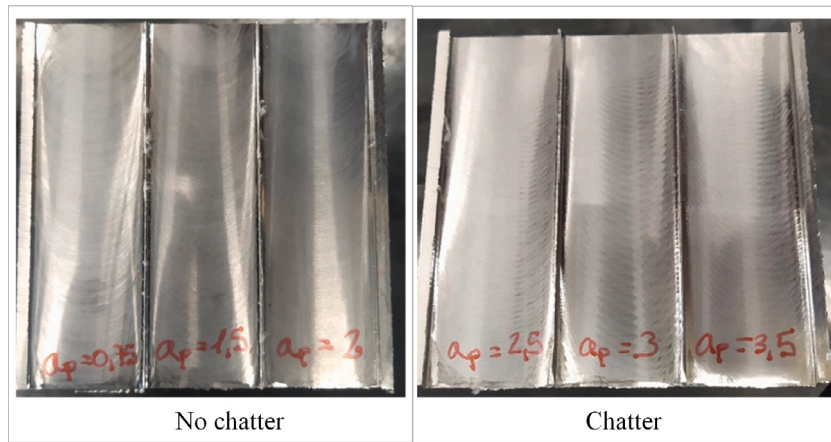


Fig. 3. Milling surfaces without chatter (left) and with chatter (right).

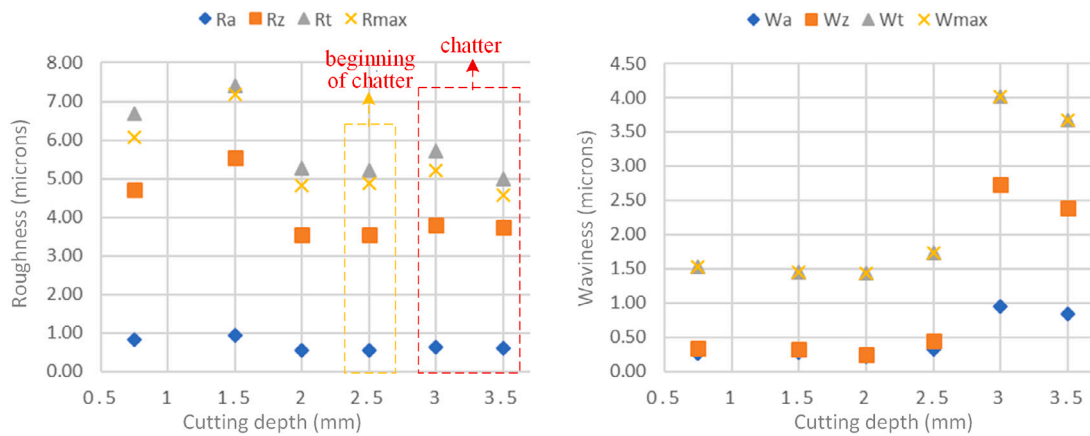


Fig. 4. Roughness (R_a , R_z , R_t , R_{max}) and waviness (W_a , W_z , W_t , W_{max}) measurement results at different cutting depths.

Table 2

Roughness and waviness measurement results of machined surfaces with different cutting depths (Units: roughness: microns, waviness: microns, cutting depth: mm).

AP	0.75		1.50		2.00		2.50		3.00		3.50	
	Avg.	SD										
R_a	0.83	0.03	0.93	0.02	0.54	0.02	0.55	0.03	0.64	0.04	0.60	0.02
R_z	4.72	0.11	5.54	0.10	3.55	0.10	3.54	0.13	3.80	0.16	3.73	0.22
R_t	6.69	0.20	7.40	0.47	5.26	0.27	5.22	0.13	5.72	0.71	5.00	0.37
R_{max}	6.08	0.33	7.19	0.35	4.83	0.28	4.88	0.27	5.22	0.70	4.58	0.27
W_a	0.26	0.00	0.28	0.03	0.22	0.02	0.33	0.04	0.94	0.24	0.83	0.13
W_z	0.34	0.04	0.33	0.11	0.24	0.04	0.44	0.14	2.73	0.83	2.39	0.22
W_t	1.54	0.05	1.46	0.09	1.44	0.18	1.73	0.12	4.02	1.03	3.67	0.72
W_{max}	1.54	0.05	1.46	0.09	1.44	0.18	1.73	0.12	4.02	1.03	3.67	0.72

4.2.1. FFT analysis

Fig. 5 shows the comparison between normal and chatter cutting status of the external accelerometer signal on one of the three axes. The time domain represents the raw data and the frequency domain represents the output of FFT. Significant difference can be identified in the frequency domain as shown in Fig. 5. Extra frequency components appear near 1100 Hz and 1200 Hz, which correspond to chatter frequencies. Similar pattern can be found in the other two accelerometer axes. This result agrees with previous studies about chatter detection that are based on accelerometer signals.

The same analysis approach is applied to the internal signals. As shown in Fig. 6, no significant extra frequency components are identified in the frequency domain with the default amplitude scale, which is different from the accelerometer signals. Similar results can be found in other internal signals. In order to obtain more chatter-related details, the internal signals are further analyzed with

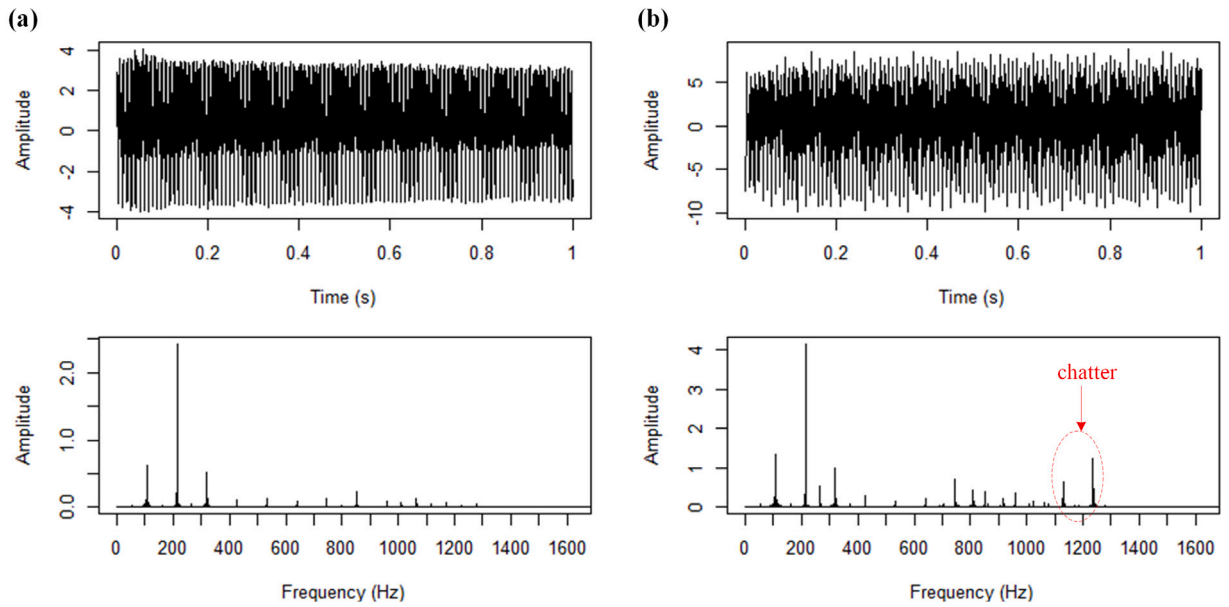


Fig. 5. External accelerometer signal (Z-axis) in time domain and frequency domain. (a) normal cutting without chatter, depth of cut: 1.50 mm; (b) cutting with chatter, depth of cut: 3.5 mm.

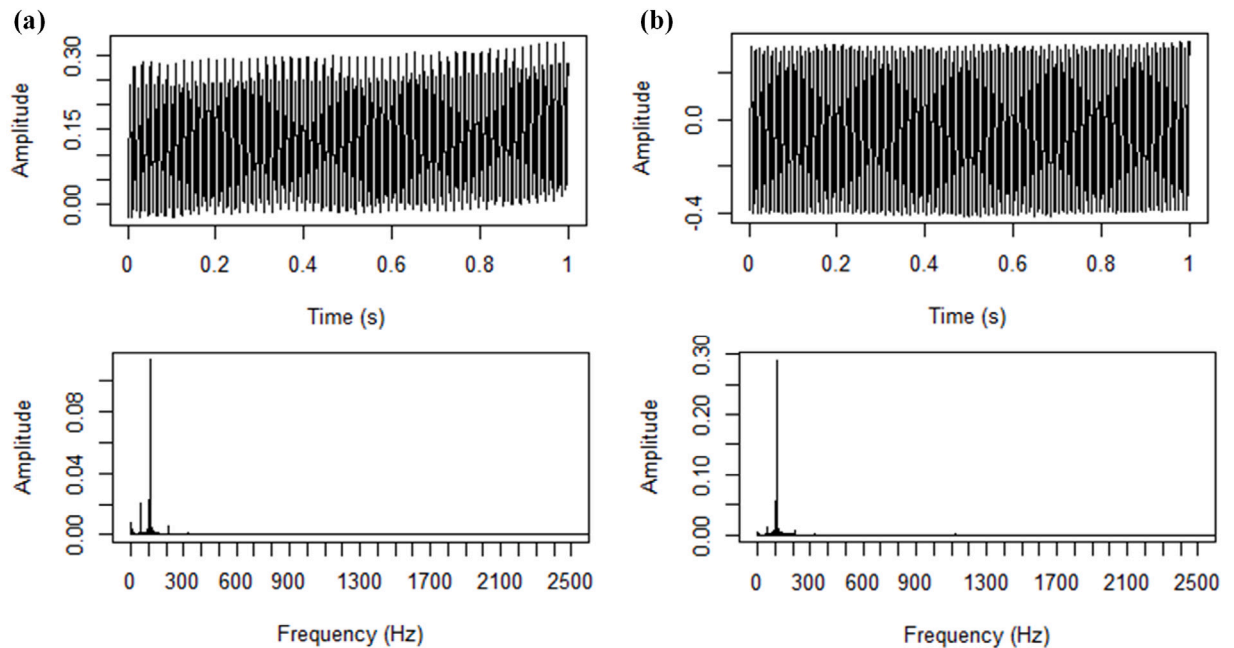


Fig. 6. Internal CNC signal (I-N-int-Z) in time domain and frequency domain. (a) normal cutting without chatter, depth of cut: 1.50 mm; (b) cutting with chatter, depth of cut: 3.5 mm.

zoomed-in scale in the frequency domain around the chatter frequencies as identified in the accelerometer signal (approx. 1125 Hz and 1230 Hz). The details of some exemplary signals (*s-act-X*, *I-N-int-X*, *I-N-int-S1*, *M-actual-S1*) are shown in Fig. 7. The results show that extra frequency components corresponding to chatter appear in some of the internal signals such as *I-N-int-S1*, *M-actual-S1* at a much smaller scale than the accelerometer signals; whereas the other internal signals, such as *s-act-X*, *I-N-int-X*, are not affected by the chatter vibrations. The possible reasons for this result include: firstly, the chatter vibrations are transmitted from the cutting tool to the spindle drive motor through the machine’s structural component chain and servo amplifiers, which can reduce and distort the vibration signals; secondly, limited by the bandwidth of the data acquisition software, the sampling frequency of some internal

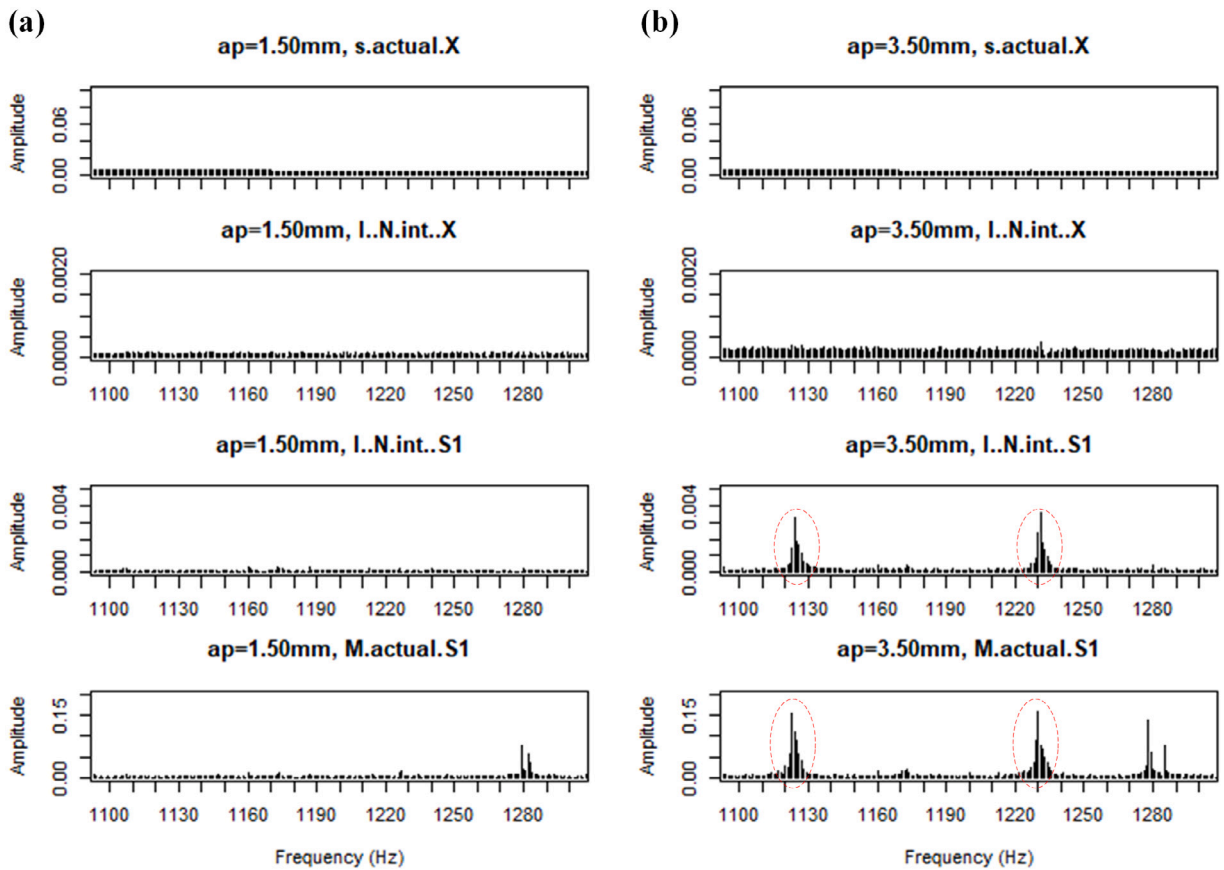


Fig. 7. Internal signals (s-act-X, I-N-int-X, I-N-int-S1, M-actual-S1) in frequency domain.(a) normal cutting without chatter, depth of cut: 1.50 mm; (b) cutting with chatter,depth of cut: 3.5 mm.

signals (the $a-act$, $v-act$ and $s-act$ signals in Table 1) is lower than the frequency of chatter vibrations ($333 \text{ Hz} < 1125 \text{ Hz}$), making them incapable of capturing the chatter characteristics.

Previous studies [1,6] have proposed to use a state observer to reduce the influence of the amplifiers and structural dynamic modes and dynamically compensate the drive motor current signals. These approaches require deep knowledge about the machine and controlling system, such as the control loop of the spindle drive and the related transfer function of the current loop. It increases the difficulty of developing chatter detection applications. The preliminary frequency analysis, as shown in Fig. 7, implies the potential of using the relevant internal signals directly for chatter detection without compensation. The following sections will investigate their performance based on popular machine learning algorithms.

4.2.2. Band-pass filtering

The raw signal captured during milling processes contains mainly three types of components: the normal periodic components caused by the rotation of the cutter, the abnormal chatter vibration components, and the stochastic perturbation components caused by system noise and inhomogeneous material etc.[8]. The main challenge of chatter detection is to distinguish it from the periodic components since their amplitudes are much higher than the noise components.

A comb filter was proved to be reliable for removing the periodic components by filtering out the spindle rotation frequency, tooth passing frequency and their harmonics [8]. It performs well to the external acceleration signals where the chatter vibrations are directly captured by the attached accelerometer. However, after tested in this study, the result is not significant when applying such a comb filter to the internal signals, possibly due to the decrease of chatter amplitude during the signal transmitting from cutting tool to drive motor. A band-pass filter is therefore applied to filter the raw signal in this study. As shown in Fig. 7, the chatter vibration components are located around 1125 Hz and 1230 Hz in the frequency domain. This has been confirmed by both external and internal signals. Therefore, a band-pass filter that passes frequencies between 1100 Hz and 1250 Hz can remove all the periodic components.

4.2.3. EEMD decomposition

The filtered signals are then decomposed with the EEMD method aiming to identify the most sensitive IMFs which can reflect the chatter information. As shown in Fig. 8, the information of external acceleration signals (X, Y, Z axes) is heavily concentrated

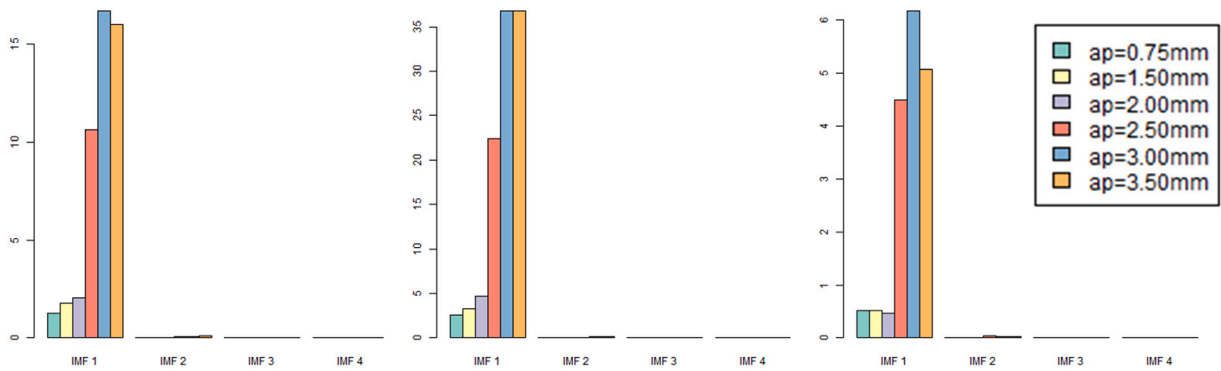


Fig. 8. Relative energy ratio of four IMFs of external accelerometer signals (X, Y, Z axes from left to right) during six cutting depths.

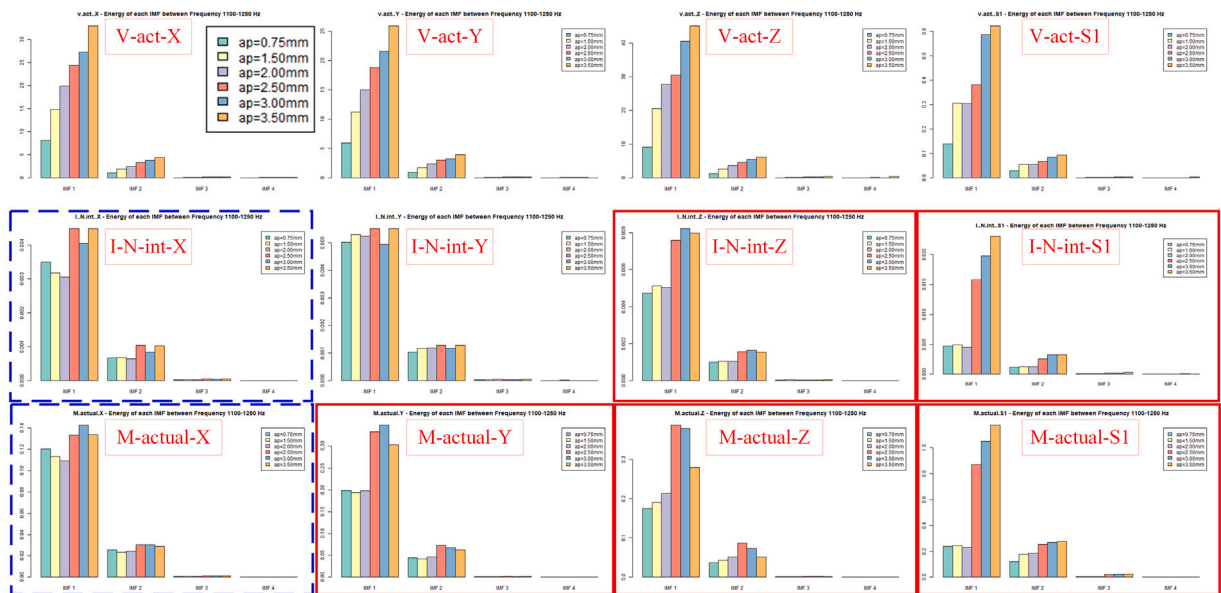


Fig. 9. Relative energy ratio of four IMFs of internal signals during different cutting depths (solid red border: significant for chatter detection; dotted blue border: possibly significant for chatter detection; no border: insignificant for chatter detection).

in IMF-1. The EEMD result indicates the significant difference between normal and chatter situations which can be used for chatter detection. It is obvious that there is a huge jump of the relative energy ratio from normal situations (three left columns) to chatter situations (three right columns).

Similar pattern occurs in EEMD results of some internal signals. As shown in Fig. 9, most of energy of internal signals is also concentrated in the first IMF. Notable differences between normal and chatter situations can also be observed in some of the signals (marked with solid red border), including I-N-int-Z, I-N-int-S1, M-actual-Y, M-actual-Z and M-actual-S1. Possible differences can be seen on some other signals (marked with dotted blue border) including I-N-int-X and M-actual-X. They need to be further evaluated to confirm their feasibility for chatter detection. The other internal signals do not show obvious differences between normal and chatter situations, thus they are excluded in the following analysis. It is worth to mention that, all the signals related to $a - act$, $v - act$ and $s - act$ (see Table 1) are insignificant for chatter identification. This result agrees with the previous FFT analysis result. The details of every plot in Fig. 9 are provided in Appendix A.

4.3. Chatter detection

4.3.1. C_0 complexity and Power Spectral Entropy

The frequency analysis and EEMD decomposition results indicate the possibility of chatter detection based on external signals and some of the internal signals. However, these results are not suitable to be used directly for automatic chatter detection. To cope with this problem, the C_0 complexity and PSE of the IMF-1 component of possible signals are calculated as key indicators for chatter. Fig. 10 shows the C_0 complexity values (solid yellow lines) and PSE values (dotted blue lines) of two signals (external

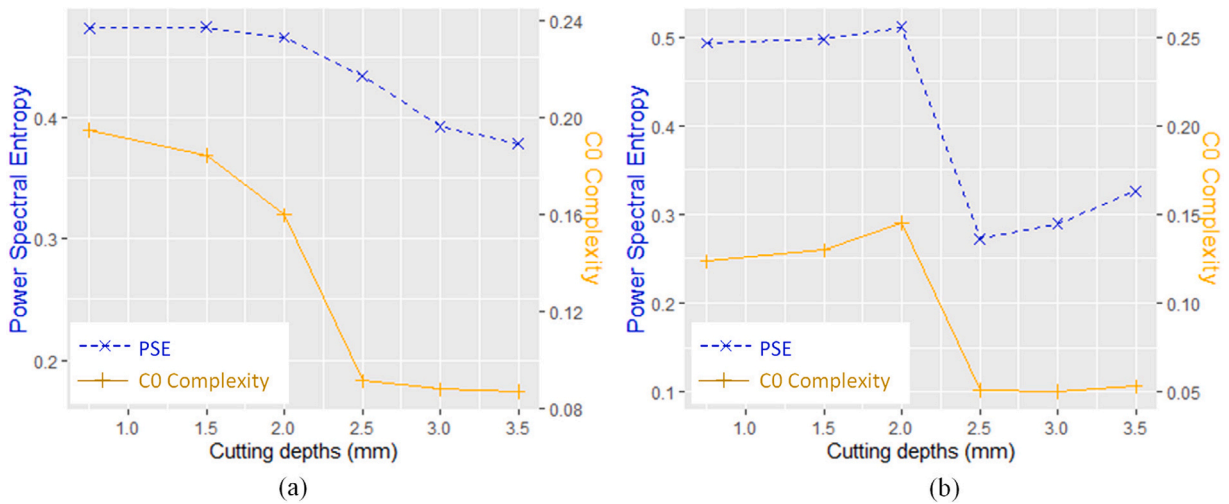


Fig. 10. C₀ complexity and Power Spectral Entropy of signals in one second: (a) external acceleration on Z-axis signal; (b) internal I-N-int-S1 signal.

Table 3
C₀ complexity of external and internal signals.

AP (mm)	External signals			Internal signals							
	Accelerometer			I N int				M actual			
	X	Y	Z	X	Y	Z	S1	X	Y	Z	S1
0.75	0.256	0.239	0.195	0.643	0.632	0.628	0.493	0.640	0.617	0.642	0.513
1.50	0.225	0.223	0.184	0.644	0.624	0.636	0.497	0.645	0.619	0.643	0.530
2.00	0.272	0.238	0.160	0.650	0.622	0.631	0.511	0.631	0.609	0.628	0.498
2.50	0.120	0.132	0.092	0.546	0.600	0.332	0.272	0.601	0.421	0.462	0.447
3.00	0.109	0.133	0.088	0.553	0.617	0.365	0.289	0.613	0.440	0.479	0.394
3.50	0.102	0.140	0.087	0.583	0.601	0.415	0.326	0.602	0.460	0.440	0.392

Table 4
Power Spectral Entropy of external and internal signals.

AP (mm)	External signals			Internal signals							
	Accelerometer			I N int				M actual			
	X	Y	Z	X	Y	Z	S1	X	Y	Z	S1
0.75	0.509	0.583	0.473	0.158	0.126	0.145	0.123	0.156	0.129	0.144	0.176
1.50	0.473	0.548	0.474	0.163	0.138	0.143	0.130	0.172	0.125	0.144	0.205
2.00	0.550	0.524	0.465	0.162	0.135	0.148	0.145	0.166	0.134	0.147	0.202
2.50	0.461	0.430	0.434	0.143	0.135	0.113	0.051	0.159	0.111	0.110	0.112
3.00	0.409	0.404	0.392	0.148	0.140	0.122	0.050	0.136	0.101	0.140	0.100
3.50	0.374	0.420	0.378	0.152	0.133	0.115	0.053	0.151	0.132	0.140	0.104

acceleration on Z-axis signal and internal I-N-int-S1 signal). The complete results of the three external signals and eight internal signals are listed in Table 3 (C₀ complexity) and Table 4 (PSE).

As shown in Fig. 10, in general, the C₀ complexity and PSE of normal situations (cutting depths 0.75, 1.50 and 2.00 mm) are much larger than chatter situations (cutting depths 2.50, 3.00 and 3.50 mm). For the external acceleration signal (10-(a)), both C₀ and PSE values decrease gradually from cutting depth 0.75 mm to 2.00 mm. Then a sharp decrease occurs from 2.00 mm to 2.5 mm, when chatter appears. Then the C₀ values decrease very slow with increasing cutting depths, while the SPE values decrease slightly faster than C₀ values. Similar results are obtained from the other two external signals (acceleration X and Y axes), as demonstrated in Tables 3 and 4. This result agrees with the previous study [8].

As to the internal signal (I-N-int-S1), a sharp decrease also occurs from 2.00 mm to 2.5 mm. The difference is that the C₀ and SPE values do not decrease inside normal situations (cutting depths 0.75, 1.50 and 2.00 mm) and chatter situations (cutting depths 2.50, 3.00 and 3.50 mm). There is even a slight increase. This might be caused by the band-pass filter, whereas the root cause need to be further investigated. This phenomenon has no impact on chatter detection, but it creates difficulties for categorizing chatters into different severity levels. As listed in Tables 3 and 4, similar patterns are observed from other internal signals such as I-N-int-Z, I-N-int-S1, M-actual-Y, M-actual-Z and M-actual-S1, whereas the other signals such as I-N-int-X, I-N-int-Y and M-actual-X shows less significant variations. This result agrees with the EEMD analysis result shown in Fig. 9.

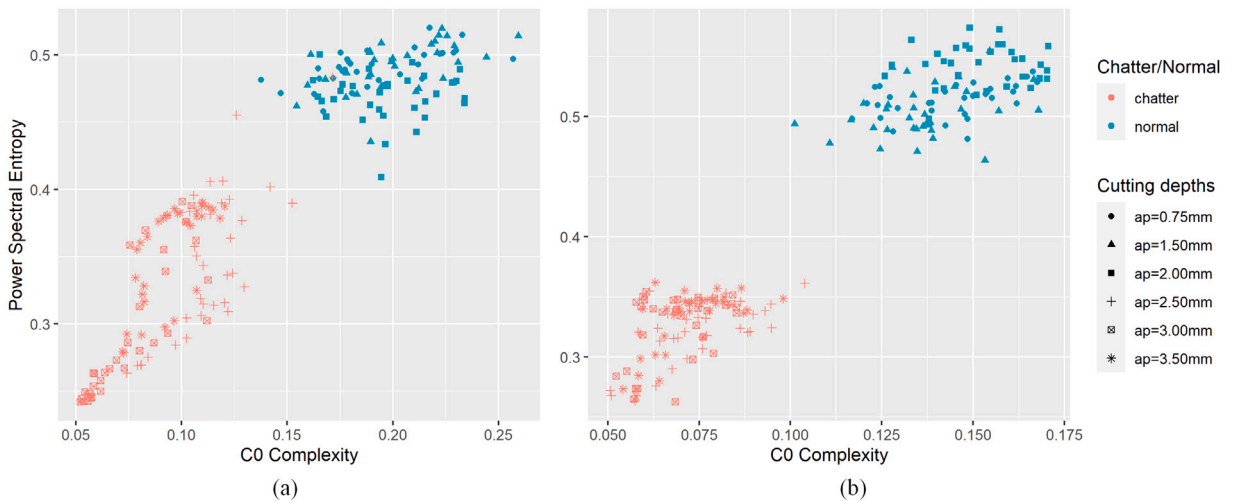


Fig. 11. Distribution of signal segments (length 0.5 s, without overlap) according to their C_0 complexity and PSE values: (a) external acceleration on Z-axis; (b) internal I-N-int-S1 signal.

The calculation results can be explained by the physical meaning of C_0 complexity and PSE indicators. The C_0 complexity represents the proportion of random components in a signal. As shown in Fig. 7, the filtered signals (between frequency 1100 Hz and 1250 Hz) consist of mainly stochastic noise during normal milling processes, thus the C_0 values are relatively high. In contrast, during the chatter situations, the filtered signals are dominated by the periodic chatter components (at approx. 1125 Hz and 1230 Hz), whereas the proportion of random components decrease correspondingly. Therefore the C_0 values drop significantly.

Similarly, the PSE indicator also reflects the uncertainty level of a signal. Higher PSE values represent higher levels of uncertainty and the frequency components distribution of the signals are comparatively even. Therefore, the PSE values of filtered normal situation signals, which contains mainly noises, are higher than the PSE values of chatter situations.

The aforementioned analysis result proves that the C_0 complexity and PSE can be used as reliable indicators for chatter identification. The combination of both indicators can differentiate chatter from stable situations which is further proved by applying them to multiple signal segments. Fig. 11 shows the distribution of C_0 and PSE values of some signal segments (acceleration Z-axis and I-N-int-S1) during the six cutting depths. The segments are obtained by cutting the original signal with a moving window (length 0.5 s, without overlap). Totally 15 segments are obtained for each signal during one cutting depth.

All the data analysis is conducted in the RStudio software on a computer equipped with Intel(R) Core(TM) i7-8565U CPU, 16 GB RAM, and a 64-bit Window 11 operating system. The average computing time for the C_0 complexity and PSE values of each external acceleration signal segment (length 0.5 s) is 0.0134 (std. 0.0008) second. The average computing time for each internal CNC signal segment (length 0.5 s) is 0.0709 (std. 0.0013) second. It is longer than the external signals because they contain more data due to higher sampling frequency.

As shown in Fig. 11, there is a clear boundary between normal and chatter situations. The normal segments are located at the bottom-left corner with smaller C_0 and PSE values, and the chatter segments at the top-right corner with larger C_0 and PSE values. The internal I-N-int-S1 signals shows even better clustering performance with this approach than the external acceleration signal. This result enables to define a threshold according to the C_0 and PSE values to indicate the occurring of chatter.

The C_0 and PSE calculation results of all the signals are presented in Appendix B. Similar to the above result, obvious boundaries can be observed in all three external acceleration signals (Appendix B - Fig. 15) and some internal signals including I-N-int-Z, I-N-int-S1, M-actual-Y, M-actual-Z and M-actual-S1 (Appendix B - Figs. 16 and 17), with a few mixed segments in some signals. In general, the internal signals obtained equivalent performance for chatter detection to the external acceleration signals. No clear gaps are found in the other internal signals, i.e. I-N-int-X, I-N-int-Y and M-actual-X. It means these signals are insignificant for chatter detection.

4.3.2. Autoencoder

The C_0 complexity and PSE approach relies on the data preprocessing, including the time–frequency analysis and filtering etc. It requires deep understanding about the chatter characteristics in order to manually extract the proper features. Machine learning algorithms such as autoencoder enables automatic feature extraction by training a neural network with historical data.

A five-layer autoencoder (number of node: 100-20-10-20-100) is built to extract features for chatter detection using the previous signal segments (length 0.5 s, without overlap). The raw data of the captured signals are the input of the autoencoder, and the labels are two-fold, i.e. “chatter” (cutting depth: 0.75, 1.5, 2.0 mm) and “normal” (cutting depth: 2.5, 3.0, 3.5 mm). The segments are split to training and testing datasets. Two different splitting trials are tested to better evaluate the performance of different signals for chatter detection.

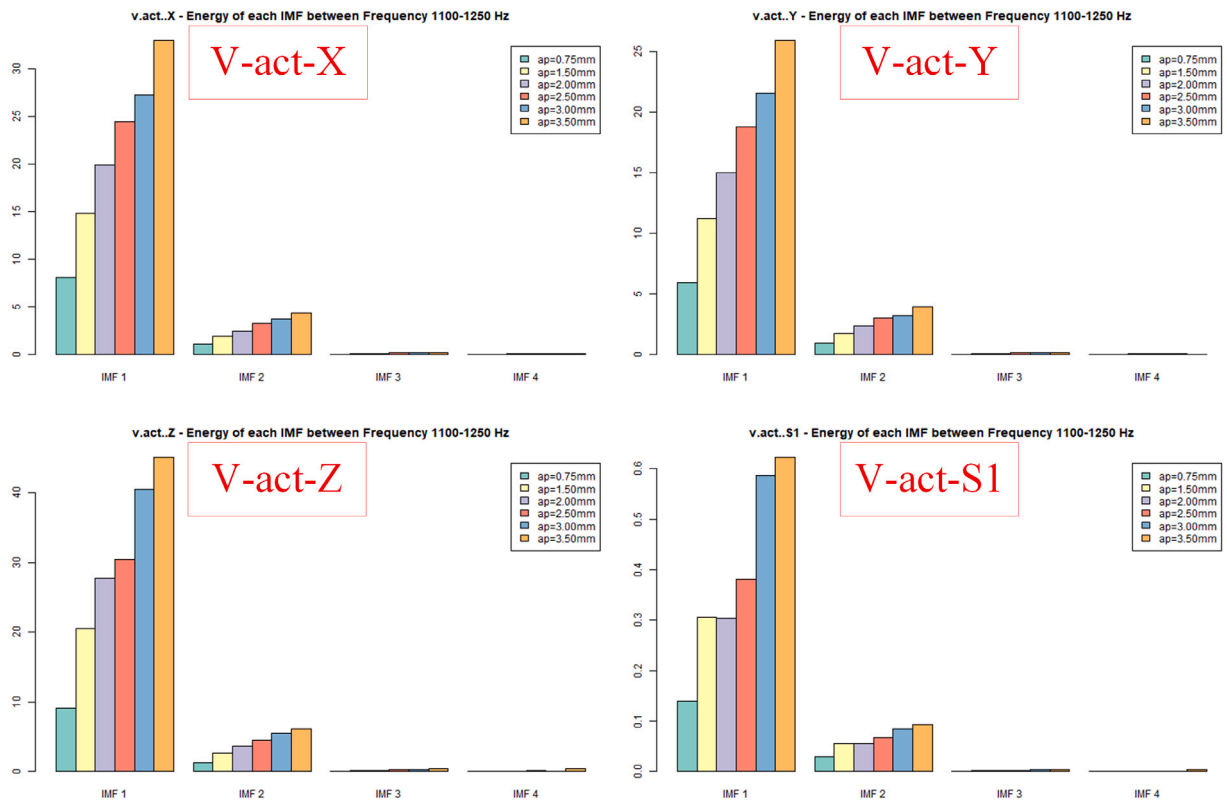


Fig. 12. Relative energy ratio of four IMFs of internal V-act signals during different cutting depths.

Table 5

Chatter prediction results based on different signals using SVM and features extracted by autoencoder (Accuracy: number of correctly predicted samples divide total number of samples; Sensitivity: number of correctly predicted chatter samples divide total number of chatter samples.).

	External signals			Internal signals							
	Accelerometer			I N int				M actual			
	X	Y	Z	X	Y	Z	S1	X	Y	Z	S1
Chatter (3.0)	15	15	15	12	6	15	15	10	15	14	12
Normal (1.5)	15	15	15	10	10	13	15	9	11	14	15
Accuracy	1.00	1.00	1.00	0.73	0.53	0.93	1.00	0.63	0.87	0.93	0.90
Sensitivity	1.00	1.00	1.00	0.80	0.40	1.00	1.00	0.67	1.00	0.93	0.80
Chatter (2.5)	13	13	14	7	6	14	13	7	14	13	10
Normal (2.0)	15	15	15	15	8	11	15	11	11	11	15
Accuracy	0.93	0.93	0.97	0.73	0.47	0.83	0.93	0.60	0.83	0.80	0.83
Sensitivity	0.87	0.87	0.93	0.47	0.40	0.93	0.87	0.47	0.93	0.87	0.67

- For the first trial the segments belonging to cutting depth 1.5 mm (normal) and 3.0 mm (chatter) are taken out as testing data. The former ones are captured during stable milling process which is still far from chatter appearance, whereas the latter ones are captured when chatter already reach a comparatively high level. These two groups are expected easier to be distinguished.
- For the second trial, the segments of cutting depth 2.0 mm (normal) and 2.5 mm (chatter) are leave out for testing. These two groups near the threshold when chatter started to occur. They are expected to be more difficult to be distinguished.

For each trial, the training samples are first used to train the autoencoder model (hyperbolic tangent activation function, 100 epochs). The ten features of the third layer are then extracted and used as input to train a SVM classifier. Finally, the trained SVM is used to predict chatter with the testing samples. The prediction results of the three externals acceleration signals and eight internal signals, including the insignificant ones according to C_0 and PSE approach, are listed in Table 5.

As shown in Table 5, the external acceleration signals correctly classified all the 30 testing samples for the first trial (cutting depth 1.5 and 3.0 mm); and misclassified two (X and Y axis) and one (Z axis) chatter samples as normal for the second trial ((cutting depth 2.0 and 2.5 mm)), achieving 93% (87%) and 97% (93%) accuracy (sensitivity) respectively.

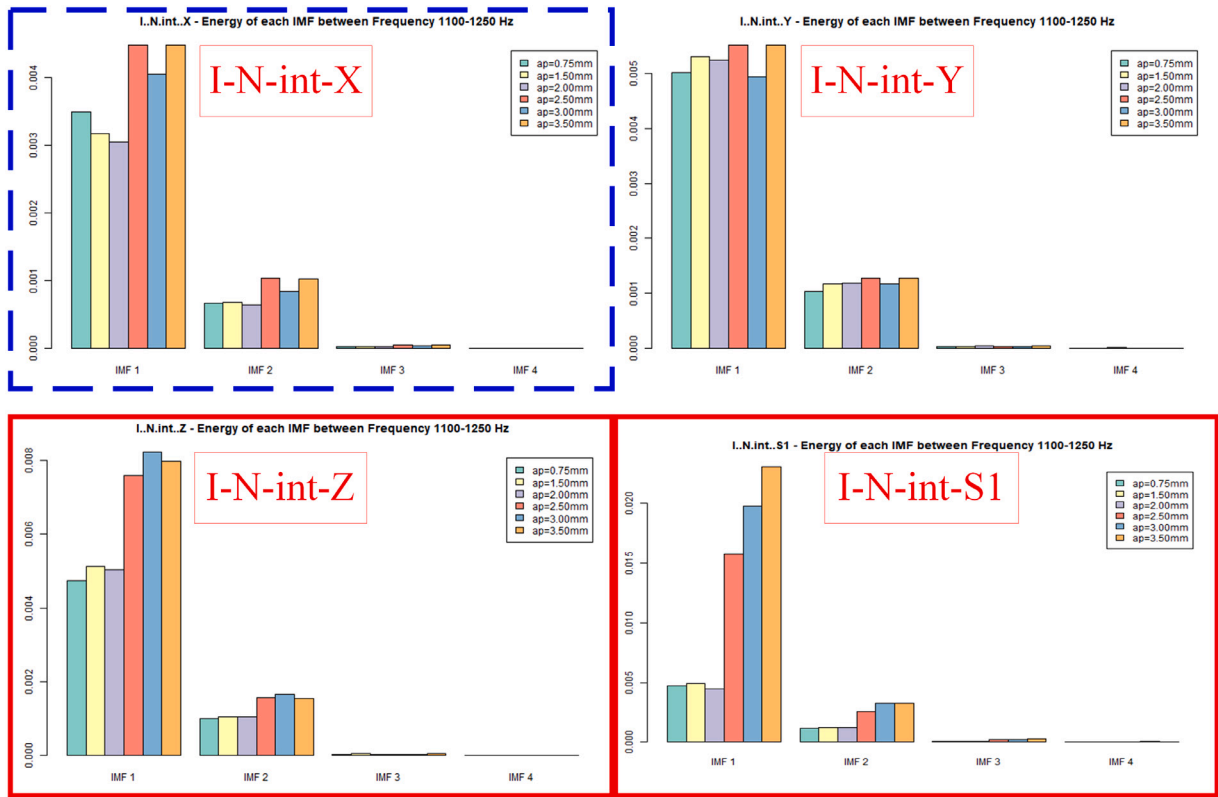


Fig. 13. Relative energy ratio of four IMFs of internal I-N-int signals during different cutting depths (solid red border: significant for chatter detection; dotted blue border: possibly significant for chatter detection; no border: insignificant for chatter detection).

As comparison, the internal signal I-N-int-S1 achieves equivalent performance as the external signals which correctly classified all testing samples for the first trial and misclassified two samples for the second trial. The signals I-N-int-Z, M-actual-Y, M-actual-Z and M-actual-S1 also obtained comparable performance achieving a minimum 87% (80%) accuracy (sensitivity) for the first trial and a minimum 80% (67%) accuracy (sensitivity) for the second trial. This result agreed with the previous C_0 and SPE calculation result, and confirmed the capability of these signals for chatter detection. No significant performance obtained from the other internal signals, i.e. I-N-int-X, I-N-int-Y and M-actual-X, meaning they are not suitable for chatter detection.

In terms of computing time, the training of corresponding autoencoder models takes longer time than the C_0 and PSE approach, whereas the prediction based on SVM takes negligible short time. In practical applications, the autoencoder models can be trained off-line in advance. More specifically, for each external acceleration signal, the average time for training the autoencoder model is 30.6449 (std. 0.0651) seconds; for training the SVM model is 0.0060 (std. 0.0013) second, and for predicting 30 segments is 0.0042 (std. 0.0004) second. For each internal CNC signal, the average time for training the autoencoder model is 93.9254 (std. 2.3022) seconds which is longer due to larger data size; for training the SVM model is 0.0053 (std. 0.0001) second, and for predicting 30 segments is 0.0046 (std. 0.0005) second. This result indicates that the autoencoder and SVM approach is much faster than the C_0 and PSE approach for on-line chatter detection once the autoencoder is pre-trained, making it more suitable for large scale production scenarios.

4.3.3. Deep Convolution Neural Networks

The two approaches introduced above are among the most popular signal processing methods for chatter detection. These two methods separate the feature extraction and chatter detection processes. Some recent studies use advanced algorithms such as deep Convolution Neural Networks (CNN) [36,37] for chatter detection without separating it with the feature extraction process. Although algorithms are not the main concern of this study, it is beneficial to explore the performance of the external and internal signals with such an algorithm. For this purpose, a four-layer CNN model is created and the same data samples (15 segments for each signal) are used for training and testing the model. The parameters of the model such as the number of nodes of each layer, dropout rate, training epochs etc., are adjusted for different signals to obtain the optimal result.

The segments of cutting depth 2.0 mm (normal) and 2.5 mm (chatter) are used for testing at this stage since they are more difficult to differentiate. The training and testing result of each signal is shown in Table 6. The training accuracy is achieved during the training process of the model using the rest of the segments; and the testing accuracy and sensitivity are the prediction result

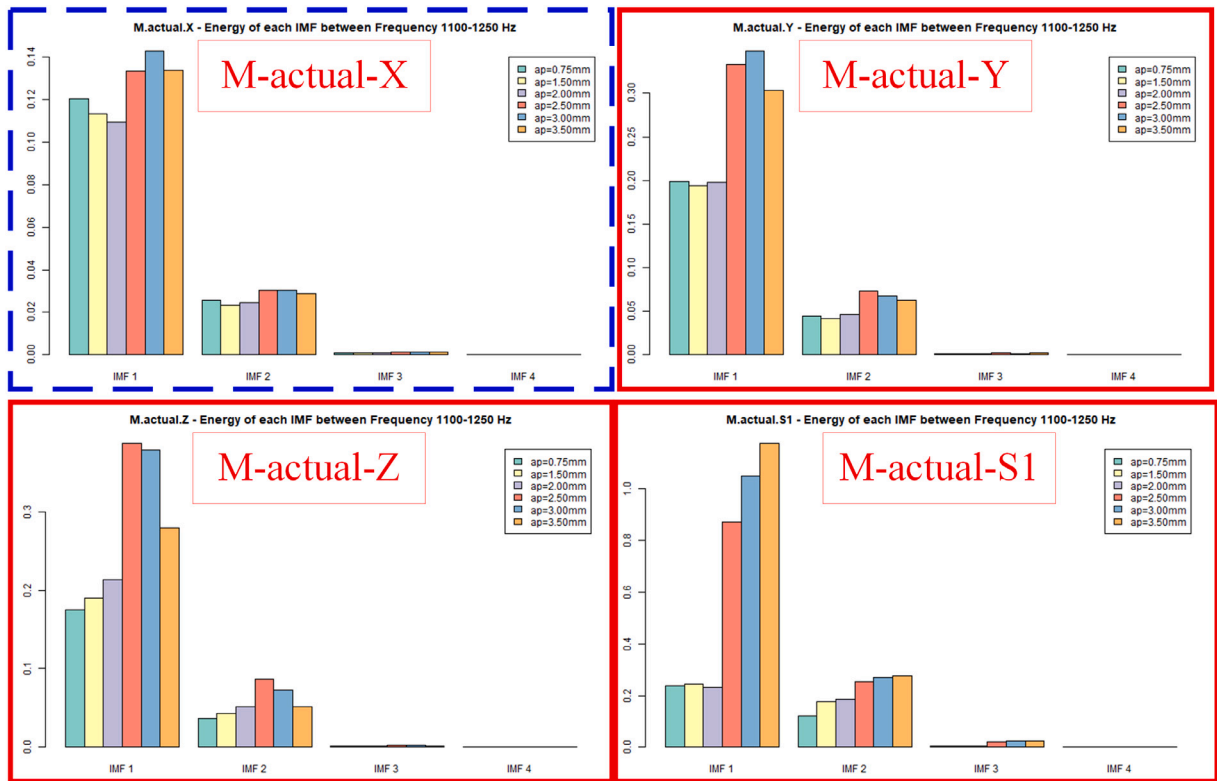


Fig. 14. Relative energy ratio of four IMFs of internal M-actual signals during different cutting depths (solid red border: significant for chatter detection; dotted blue border: possibly significant for chatter detection; no border: insignificant for chatter detection).

Table 6

Chatter prediction results based on different signals using Convolution Neural Networks (Accuracy: number of correctly predicted samples divide total number of samples; Sensitivity: number of correctly predicted chatter samples divide total number of chatter samples.).

	External signals			Internal signals							
	Accelerometer			I N int				M actual			
	X	Y	Z	X	Y	Z	S1	X	Y	Z	S1
Chatter (2.5)	10	10	12	5	7	12	9	5	4	4	6
Normal (2.0)	15	15	15	14	12	15	15	11	15	15	15
Training acc.	0.94	0.98	0.99	0.85	0.89	0.98	0.96	0.89	0.81	0.95	0.93
Testing acc.	0.83	0.83	0.90	0.63	0.63	0.90	0.80	0.53	0.63	0.63	0.70
Sensitivity	0.67	0.67	0.80	0.33	0.47	0.80	0.60	0.33	0.27	0.27	0.40

for normal (2.0 mm) and chatter (2.5 mm) situations. Due to limited number of training samples, both the internal and external signals produced lower accuracy and sensitivity than the previous SVM method. The external Z-axis acceleration signal and internal signal I-N-int-Z obtained the best performance with 90% accuracy and 80% sensitivity. Different from the previous two methods, the internal signal I-N-int-S1 produced relatively lower performance with 80% accuracy and 60% sensitivity, which is similar to external acceleration X and Y signals. The performance of the rest internal signals is not as good as in the previous methods.

4.4. Discussion

The experiment results proved that internal CNC signals can achieve satisfying performance for chatter detection with both conventional and automatic feature extraction methods. The internal signals have different levels of capabilities for chatter detection. The CNC current signal I-N-int-S1 and I-N-int-Z achieved equivalent performance to the external acceleration signals. This agrees with the fact that chatter vibrations has larger amplitude on the Z axis which is vertical to the machining plane. The torque signals M-actual-Y, M-actual-Z and M-actual-S1 also obtained satisfying performance with the C₀ and PSE approach, as well as autoencoder and SVM approach, although they produced imperfect results with CNN method due to limited training dataset.

As a complement of this study, the CNN method was also explored preliminarily which produced lower performance for both internal and external signals. The main reason is that the training dataset is too small. Only small amount of data samples are

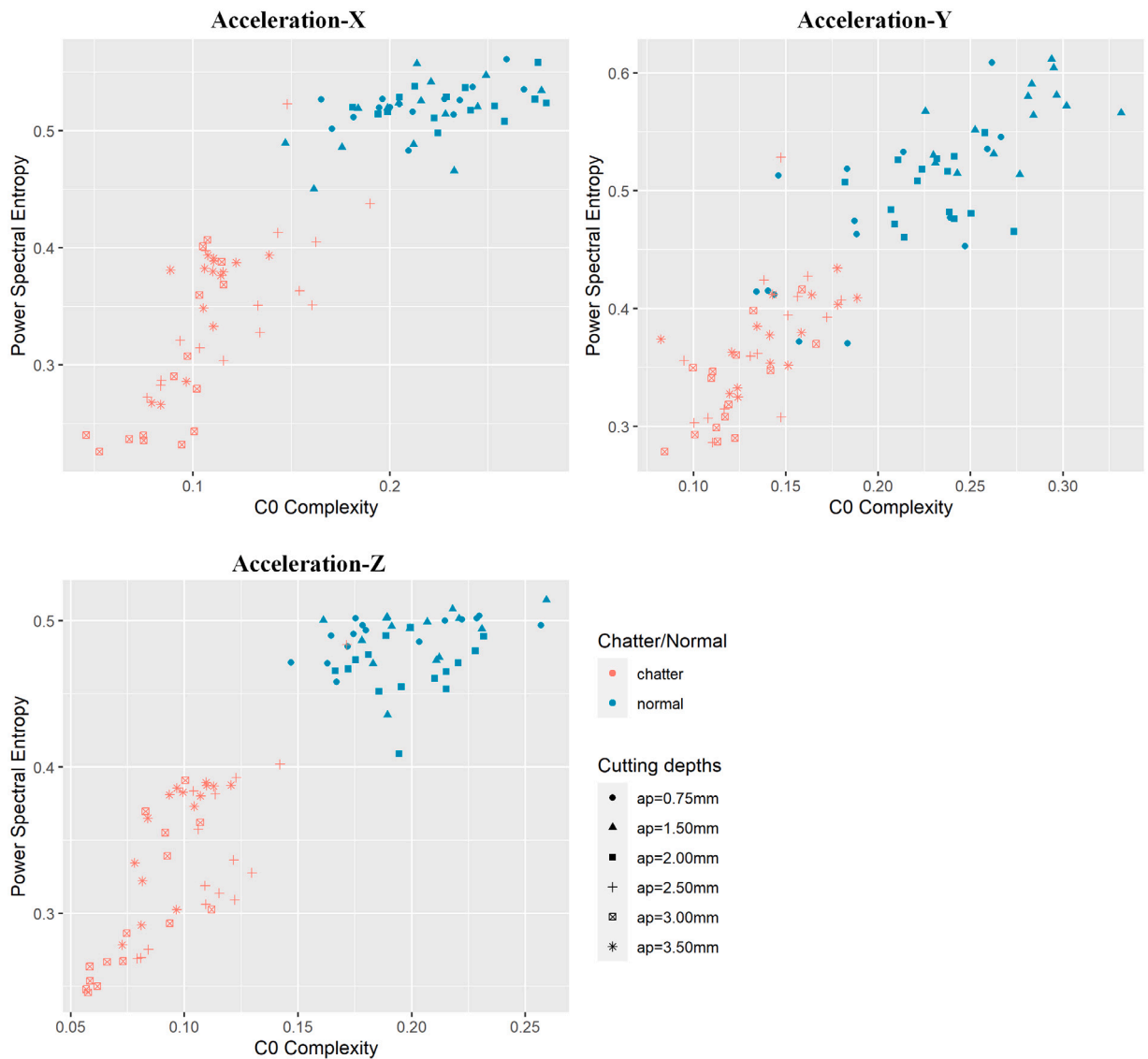


Fig. 15. Distribution of signal segments (length 0.5 s, without overlap) according to their C_0 complexity and PSE values: external acceleration on X, Y and Z axis.

collected since the algorithm is not the main concern of this study. However, this primary exploration demonstrates the feasibility of using internal signals for chatter detection with CNN method, since at least two of the internal signals, i.e. I-N-int-Z and I-N-int-S1, achieved comparable results with external signals. In practical applications, the performance of internal signals can be significantly improved by increasing the number of training samples and optimizing the parameters of the CNN models.

5. Conclusion

This paper investigated the effectiveness of multiple internal CNC system signals of a milling machine for tool-workpiece couple chatter detection, and compared them with external acceleration signals captured directly from the workpiece. The FFT and EEMD methods were used to explore the time–frequency characteristics of those signals. Two chatter detection approaches were verified based on manually extracted features and automatic features extracted with the autoencoder algorithm. The CNN method was also investigated as a complement. This study proved that the signals extracted from the inherent CNC system can be used to replace external signals for online chatter detection. It could avoid the installation of extra devices thus to reduce cost and improve production efficiency.

Due to limited resources, this paper could not cover all the aspects involved in chatter detection using internal signals. There are still some problems remained to be addressed in future studies:

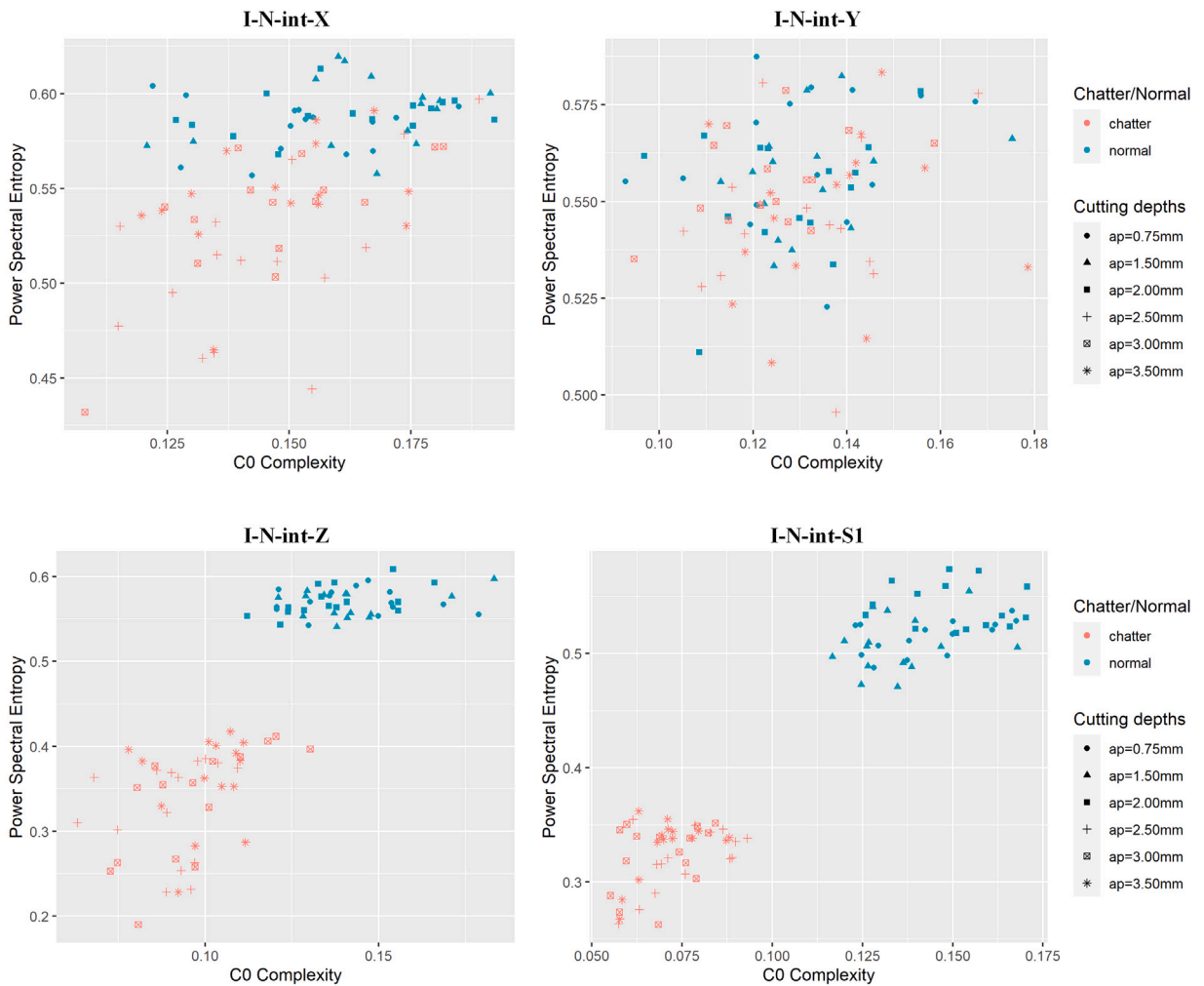


Fig. 16. Distribution of signal segments (length 0.5 s, without overlap) according to their C_0 complexity and Power Spectral Entropy values: internal I-N-int signals.

- Only the cutting depth was changed during the experiments whereas the other cutting parameters remain the same such as workpiece material, spindle speed and feed rate per tooth etc. These parameters might impact the performance of different internal signals for chatter detection. More experiments need to be conducted in future to obtain a more comprehensive result.
- The spindle drive system and relevant control loop of the milling machine were not analyzed in this paper, which is essential for explaining the performance of different signals. Such analysis need to be integrated in future studies. Similar experiments can be conducted with other machines and CNC systems.
- In addition to accelerometer, there are many other sensors that are widely used, such as acoustic and force sensors. The internal signals need to be compared with them to obtain a more reliable result.
- More advanced algorithms can be adopted to analyze the internal signals. It will require more complete experiments with longer machining time and more changing variables to produce a large amount of data samples for training different models.

Declaration of competing interest

The authors declare the following financial interests/personal relationships which may be considered as potential competing interests: Xiaochen Zheng reports financial support was provided by European Union. Dimitris Kirtsis reports financial support was provided by European Union. Pedro Arrazola reports financial support was provided by Basque Government. Daniel Echebarria reports financial support was provided by Basque Government. Patxi Aristmuno reports financial support was provided by Basque Government. Mikel Saez de Buruaga reports financial support was provided by Basque Government.

Data availability

Data will be made available on request.

Acknowledgments

The authors hereby thank the EU H2020 project QU4LITY (GA:825030 - Digital Reality in Zero Defect Manufacturing) and the Elkartek project INTOOL II (KK-2020/00103) for their financial support to this research work.

Appendix A. Relative energy ratio of four IMFs of internal signals during different cutting depths

See Figs. 12–14.

Appendix B. C_0 complexity and PSE values of different signal segments

See Figs. 15–17.

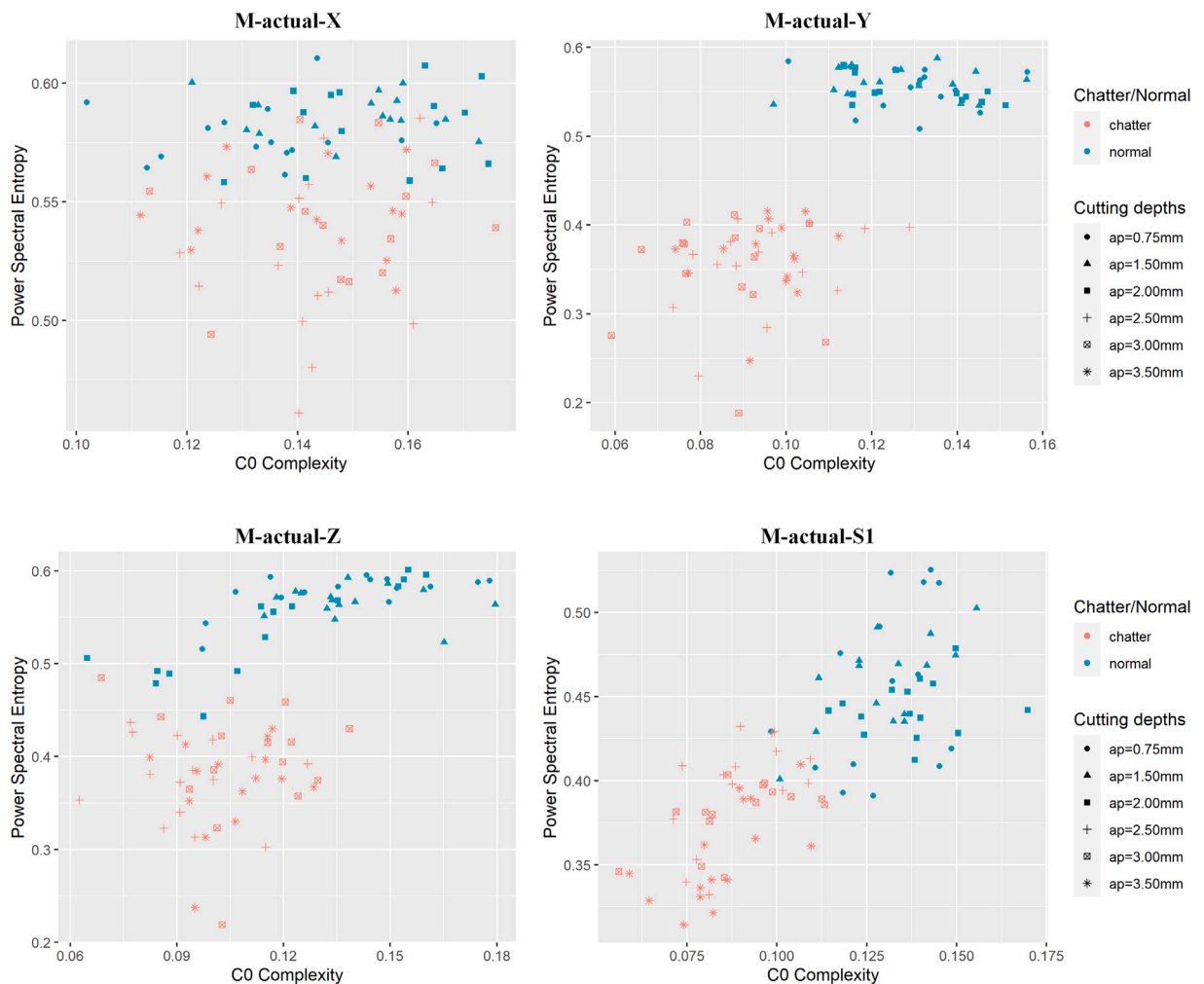


Fig. 17. Distribution of signal segments (length 0.5 s, without overlap) according to their C_0 complexity and PSE values: internal M-actual signals.

References

- [1] D. Aslan, Y. Altintas, On-line chatter detection in milling using drive motor current commands extracted from CNC, *Int. J. Mach. Tools Manuf.* 132 (2018) 64–80, <http://dx.doi.org/10.1016/j.ijmachtools.2018.04.007>.
- [2] H. Liu, Q. Chen, B. Li, X. Mao, K. Mao, F. Peng, On-line chatter detection using servo motor current signal in turning, *Sci. China Technol. Sci.* 54 (12) (2011) 3119–3129, <http://dx.doi.org/10.1007/s11431-011-4595-6>.
- [3] Y. Altintas, P.K. Chan, In-process detection and suppression of chatter in milling, *Int. J. Mach. Tools Manuf.* 32 (3) (1992) 329–347, [http://dx.doi.org/10.1016/0890-6955\(92\)90006-3](http://dx.doi.org/10.1016/0890-6955(92)90006-3).
- [4] H. Cao, Y. Yue, X. Chen, X. Zhang, Chatter detection in milling process based on synchrosqueezing transform of sound signals, *Int. J. Adv. Manuf. Technol.* 89 (9) (2017) 2747–2755, <http://dx.doi.org/10.1007/s00170-016-9660-7>.
- [5] Z. Xie, Y. Lu, J. Li, Development and testing of an integrated smart tool holder for four-component cutting force measurement, *Mech. Syst. Signal Process.* 93 (2017) 225–240, <http://dx.doi.org/10.1016/j.ymsp.2017.01.038>.
- [6] S.S. Park, Y. Altintas, Dynamic compensation of spindle integrated force sensors with Kalman filter, *J. Dyn. Sys. Meas. Control.* 126 (3) (2004) 443–452, <http://dx.doi.org/10.1115/1.1789531>.
- [7] L. Zhu, C. Liu, Recent progress of chatter prediction, detection and suppression in milling, *Mech. Syst. Signal Process.* 143 (2020) 106840, <http://dx.doi.org/10.1016/j.ymsp.2020.106840>.
- [8] H. Cao, K. Zhou, X. Chen, Chatter identification in end milling process based on EEMD and nonlinear dimensionless indicators, *Int. J. Mach. Tools Manuf.* 92 (2015) 52–59, <http://dx.doi.org/10.1016/j.ijmachtools.2015.03.002>.
- [9] D. Chen, X. Zhang, H. Zhao, H. Ding, Development of a novel online chatter monitoring system for flexible milling process, *Mech. Syst. Signal Process.* 159 (2021) 107799, <http://dx.doi.org/10.1016/j.ymsp.2021.107799>.
- [10] C. Liu, L. Zhu, C. Ni, The chatter identification in end milling based on combining EMD and WPD, *Int. J. Adv. Manuf. Technol.* 91 (9) (2017) 3339–3348, <http://dx.doi.org/10.1007/s00170-017-0024-8>.
- [11] G. Wang, H. Dong, Y. Guo, Y. Ke, Early chatter identification of robotic boring process using measured force of dynamometer, *Int. J. Adv. Manuf. Technol.* 94 (1) (2018) 1243–1252, <http://dx.doi.org/10.1007/s00170-017-0941-6>.
- [12] T. Schmitz, K. Medicus, B. Dutterer, Exploring once-per-revolution audio signal variance as a chatter indicator, *Mach. Sci. Technol.* 6 (2) (2002) 215–233, <http://dx.doi.org/10.1081/MST-120005957>.
- [13] T. Thaler, P. Potočník, I. Bric, E. Govekar, Chatter detection in band sawing based on discriminant analysis of sound features, *Appl. Acoust.* 77 (2014) 114–121, <http://dx.doi.org/10.1016/j.apacoust.2012.12.004>.
- [14] H. Sun, X. Zhang, J. Wang, Online machining chatter forecast based on improved local mean decomposition, *Int. J. Adv. Manuf. Technol.* 84 (5) (2016) 1045–1056, <http://dx.doi.org/10.1007/s00170-015-7785-8>.
- [15] S. Wan, X. Li, Y. Yin, J. Hong, Milling chatter detection by multi-feature fusion and adaboost-SVM, *Mech. Syst. Signal Process.* 156 (2021) 107671, <http://dx.doi.org/10.1016/j.ymsp.2021.107671>.
- [16] R. Koike, K. Ohnishi, T. Aoyama, A sensorless approach for tool fracture detection in milling by integrating multi-axial servo information, *CIRP Annals* 65 (1) (2016) 385–388, <http://dx.doi.org/10.1016/j.cirp.2016.04.101>.
- [17] K. Zhu, B. Vogel-Heuser, Sparse representation and its applications in micro-milling condition monitoring: noise separation and tool condition monitoring, *Int. J. Adv. Manuf. Technol.* 70 (1) (2014) 185–199, <http://dx.doi.org/10.1007/s00170-013-5258-5>.
- [18] E. Soliman, F. Ismail, Chatter detection by monitoring spindle drive current, *Int. J. Adv. Manuf. Technol.* 13 (1) (1997) 27–34, <http://dx.doi.org/10.1007/BF01179227>.
- [19] M. Lamraoui, M. El Badaoui, F. Guillet, Chatter detection in CNC milling processes based on Wiener-SVM approach and using only motor current signals, in: *Vibration Engineering and Technology of Machinery*, Springer, 2015, pp. 567–578, http://dx.doi.org/10.1007/978-3-319-09918-7_50.
- [20] K. Ohnishi, N. Matsui, Y. Hori, Estimation, identification, and sensorless control in motion control system, *Proc. IEEE* 82 (8) (1994) 1253–1265, <http://dx.doi.org/10.1109/5.301687>.
- [21] T. Yoneoka, Y. Kakinuma, K. Ohnishi, T. Aoyama, Disturbance observer-based in-process detection and suppression of chatter vibration, *Procedia Cirp* 1 (2012) 44–49, <http://dx.doi.org/10.1016/j.procir.2012.04.006>.
- [22] C. Van Loan, *Computational Frameworks for the Fast Fourier Transform*, SIAM, 1992.
- [23] N.E. Huang, Z. Shen, S.R. Long, M.C. Wu, H.H. Shih, Q. Zheng, N.-C. Yen, C.C. Tung, H.H. Liu, The empirical mode decomposition and the Hilbert spectrum for nonlinear and non-stationary time series analysis, *Proc. R. Soc. Lond. Ser. A Math. Phys. Eng. Sci.* 454 (1971) (1998) 903–995, <http://dx.doi.org/10.1098/rspa.1998.0193>.
- [24] Y. Lei, Z. He, Y. Zi, Application of the EEMD method to rotor fault diagnosis of rotating machinery, *Mech. Syst. Signal Process.* 23 (4) (2009) 1327–1338, <http://dx.doi.org/10.1016/j.ymsp.2008.11.005>.
- [25] H. Wang, J. Chen, G. Dong, Feature extraction of rolling bearing's early weak fault based on EEMD and tunable Q-factor wavelet transform, *Mech. Syst. Signal Process.* 48 (1–2) (2014) 103–119, <http://dx.doi.org/10.1016/j.ymsp.2014.04.006>.
- [26] P. Flandrin, G. Rilling, P. Goncalves, Empirical mode decomposition as a filter bank, *IEEE Signal Process. Lett.* 11 (2) (2004) 112–114, <http://dx.doi.org/10.1109/LSP.2003.821662>.
- [27] P.J. Luukko, J. Helske, E. Räsänen, Introducing libeemd: A program package for performing the ensemble empirical mode decomposition, *Comput. Statist.* 31 (2) (2016) 545–557, <http://dx.doi.org/10.1007/s00180-015-0603-9>.
- [28] C. Fang, G. Fanji, X. Jinghua, L. Zengrong, L. Ren, A new measurement of complexity for studying EEG mutual information, *Shengwu Wuli Xuebao* 14 (3) (1998) 508–512.
- [29] S. En-hua, C. Zhi-jie, G. Fan-ji, Mathematical foundation of a new complexity measure, *Appl. Math. Mech.* 26 (9) (2005) 1188–1196, <http://dx.doi.org/10.1007/BF02507729>.
- [30] Z. Cai, J. Sun, Convergence of C0 complexity, *Int. J. Bifurc. Chaos Appl. Sci. Eng.* 19 (03) (2009) 977–992, <http://dx.doi.org/10.1142/S0218127409023408>.
- [31] P. Neelakanta, J. Kapur, H. Kesavan, *Entropy Optimization Principles with Applications*, Academic press/Harcourt Brace Jovanovich publishers, Boston, MA, 1992.
- [32] A. Zhang, B. Yang, L. Huang, Feature extraction of EEG signals using power spectral entropy, in: *2008 International Conference on BioMedical Engineering and Informatics*, Vol. 2, IEEE, 2008, pp. 435–439, <http://dx.doi.org/10.1109/BMEI.2008.254>.
- [33] J.-l. Shen, J.-w. Hung, L.-s. Lee, Robust entropy-based endpoint detection for speech recognition in noisy environments, in: *ICSLP*, Vol. 98, 1998, pp. 232–235.
- [34] Y. Dun, L. Zhu, B. Yan, S. Wang, A chatter detection method in milling of thin-walled TC4 alloy workpiece based on auto-encoding and hybrid clustering, *Mech. Syst. Signal Process.* 158 (2021) 107755, <http://dx.doi.org/10.1016/j.ymsp.2021.107755>.
- [35] I. Kvinevskiy, S. Bedi, S. Mann, Detecting machine chatter using audio data and machine learning, *Int. J. Adv. Manuf. Technol.* 108 (11) (2020) 3707–3716, <http://dx.doi.org/10.1007/s00170-020-05571-9>.
- [36] M.-Q. Tran, M.-K. Liu, Q.-V. Tran, Milling chatter detection using scalogram and deep convolutional neural network, *Int. J. Adv. Manuf. Technol.* 107 (3) (2020) 1505–1516, <http://dx.doi.org/10.1007/s00170-019-04807-7>.
- [37] B. Sener, M.U. Gudelek, A.M. Ozbayoglu, H.O. Unver, A novel chatter detection method for milling using deep convolution neural networks, *Measurement* 182 (2021) 109689, <http://dx.doi.org/10.1016/j.measurement.2021.109689>.